PROCEEDINGS OF SCIENCE

Can Pions and Weak Magnetism in $2\nu\beta\beta$ Tell Us Something About BSM Physics?

Saad el Morabit,[a,b,*] **Ryan Bouabid,**[c] **Vincenzo Cirigliano,**[d] **Jordy de Vries,**[a,b] **Lukáš Gráf**[b,e] **and Emanuele Mereghetti**[f]

[a] *Institute for Theoretical Physics Amsterdam, University of Amsterdam, Science Park 904 1098 XH, Amsterdam, The Netherlands*
[b] *Theory Group, Nikhef, Science Park 105 1098 XG, Amsterdam, The Netherlands*
[c] *Department of Physics, Duke University, Durham, NC, 27708, USA*
[d] *Institute for Nuclear Theory, University of Washington, Seattle WA 98195-1550, USA*
[e] *Institute of Particle and Nuclear Physics, Faculty of Mathematics and Physics, Charles University in Prague, V Holešovičkách 2, 180 00 Praha 8, Czech Republic*
[f] *Theoretical Division, Los Alamos National Laboratory, Los Alamos, NM 87545, USA*
E-mail: s.elmorabit@nikhef.nl, ryan.bouabid@duke.edu, cirigv@uw.edu, j.devries4@uva.nl, lukas.graf@nikhef.nl, emereghetti@lanl.gov

With experiments improving their $2\nu\beta\beta$ measurements, there is growing demand for precision in its theoretical calculation. A correction that has been applied to single β-decay and $0\nu\beta\beta$, but not yet to $2\nu\beta\beta$, is the chiral correction. This correction includes the chiral potential generated by pion exchange, and the addition of weak nuclear magnetism. We show that the chiral potential reduces the half life by a few percent, which may be experimentally determined once NME uncertainties have sufficiently decreased. We also show that the weak magnetic correction modifies the spectral shape at the sub-percent level. Which ought to be included in future high-precision measurements of ξ_{31} and ξ_{51}, as well as in certain BSM scenarios, such as those involving sterile neutrinos.

Matrix Elements for the Double beta decay EXperiments (MEDEX2025)
23–27 June 2025
Czech Technical University in Prague, Prague, Czech Republic

*Speaker

ISSN 1824-8039. Published by SISSA Medialab. https://pos.sissa.it/

PoS(MEDEX2025)004

1. Introduction

As existing two-neutrino double beta decay ($2\nu\beta\beta$) measurements continue to improve, and new nuclear transitions are added to the roster, there is a growing demand for precision $2\nu\beta\beta$ spectra. The Standard Model (SM) $2\nu\beta\beta$ decay is important for studies of Beyond the Standard Model (BSM) neutrinoless double beta decay ($0\nu\beta\beta$), as it serves both as a background for $0\nu\beta\beta$ measurements and as a benchmark for testing nuclear models, which can differ by up to an order of unity in their Nuclear Matrix Elements (NMEs) [2]. Whereas $2\nu\beta\beta$ produces a broad spectrum of the order of $O(\text{MeV})$, with a typical half-life of up to $\sim O(10^{21}\ \text{yr})$, $0\nu\beta\beta$ yields a sharp peak near the $2\nu\beta\beta$ endpoint, with a half-life on the order of $\sim O(10^{26}\ \text{yr})$ or greater [1].

Precision spectral calculations require accurate accounting not only for the electromagnetic attraction between the nucleus and the outgoing electrons, but also for a distinct type of *chiral correction* that has already been applied to $0\nu\beta\beta$ and single β-decay [3–6]. These corrections employ a low-energy Effective Field Theory (EFT) for QCD called Chiral Perturbation Theory (χPT), which at next-to-leading order (NLO) for $2\nu\beta\beta$, includes Feynman diagrams where the nuclei exchange pions, as well as diagrams with vertices containing a weak magnetic component.

In this proceeding, we describe the effect of these corrections on the decay rates and energy spectra of ^{136}Xe and ^{76}Ge. We compare the size of these contributions to the NME uncertainties and to BSM effects, such as sterile neutrinos. The accompanying paper [7] on the correction also considers other BSM models and shows that these effects are of roughly the same order of magnitude for other isotopes, such as ^{100}Mo.

2. The (Differential) Decay Rate

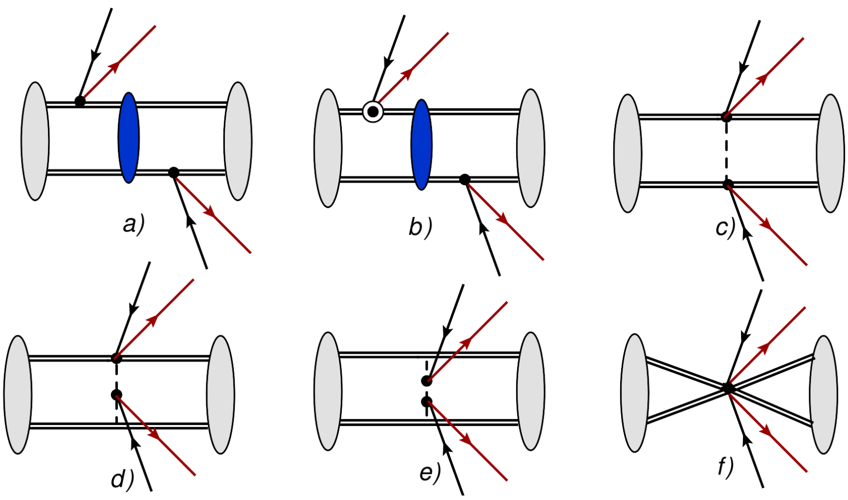

Figure 1: The Feynman diagrams. Diagram a) results in the standard $2\nu\beta\beta$ process, while diagram b) includes a weak magnetic component at one of its vertices. Diagrams c) to e) are pion exchange diagrams which, in contrast to the LO diagram, do not involve intermediate nuclear states (visualized with a blue ellipse). Diagram f) is a counterterm diagram that cancels the divergence arising from diagrams c) to e).

We only concern ourselves with the dominant ground-state to ground-state transition: $0^+ \to 0^+$ for brevity. This transition is traditionally modeled through perturbation theory in quantum mechanics, but can also be described using Chiral EFT (χEFT):

$$\begin{aligned}\mathcal{L}_{\pi N}+\mathcal{L}_{\pi}&=\bar{N}\left([ig_V v\cdot D+g_A S\cdot u]-\frac{g_M}{4m_N}\epsilon^{\mu\nu\alpha\beta}v_\alpha S_\beta f^{+}_{\mu\nu}\right)N+\frac{F_\pi^2}{4}\mathrm{Tr}\left(\left(D_\mu U\right)^\dagger D^\mu U\right)\ ,\\ l^\mu&=-2\sqrt{2}G_F V_{ud}\bar{e}_L\gamma^\mu\nu_L\tau^+ + h.c.\ ,\ U=u^2=\exp\left(i\frac{\pi\cdot\tau}{F_\pi}\right)\ .\end{aligned}\tag{1}$$

Here, l^μ is the weak current coupling to the nucleon field N and pion field π, with a coupling strength of $G_F V_{ud}$. We define $v^\mu=(1,\mathbf{0})$, $S=(0,\boldsymbol{\sigma}/2)$, τ, and m_N as the nuclear velocity, spin, isospin, and mass. The nuclei couple with respect to the vector, axial-vector, and magnetic coupling constants: $g_V=1$, $g_A=1.27$, and $g_M=4.7$. Pions couple to themselves and to nucleons with respect to the pion decay constant $F_\pi=92.2$ MeV, with the typical momentum transfer k_F of the same order as the pion mass, $k_F\sim m_\pi\sim 100$ MeV. The weak current couples through the connection Γ within the covariant derivative $D=\partial+\Gamma$, the vierbein u^μ, and $f_{\mu\nu}$, resulting in a hadronic current: $J^\mu=[g_V v^\mu-2g_A S^\mu]+ig_M m_N^{-1}\epsilon^{\mu\nu\alpha\beta}q_\nu v_\alpha S_\beta$, with $q^\mu=p^\mu-p'^\mu$ the nuclear momentum transfer. The term in square brackets in our Lagrangian and hadronic current is the LO contribution that reproduces the standard spectrum in the literature; the remaining terms are NLO. Together, they yield a decay rate:

$$\begin{aligned}\Gamma=&\frac{(G_F V_{ud})^4}{8\pi^7 m_e^2}\int_{m_e}^{E_i-E_f-m_e}\mathrm{d}E_{e1}\int_{m_e}^{E_i-E_f-E_{e1}}\mathrm{d}E_{e2}\int_{m_e}^{E_i-E_f-E_{e1}-E_{e2}}\mathrm{d}E_{\nu1}\\ &\times E_{e1}\left|\mathbf{p}_{e1}\right|E_{e2}\left|\mathbf{p}_{e2}\right|E_{\nu1}^2E_{\nu2}^2F\left(E_{e1},Z_f\right)F\left(E_{e2},Z_f\right)\frac{g_A^4}{3}\left(\left[\left(M^K_{GT}\right)^2+\left(M^L_{GT}\right)^2+M^K_{GT}M^L_{GT}\right]\right.\\ &\left.\times\left(1-\frac{2g_M}{3m_N g_A}\left(Q+2m_e-(E_{e1}+E_{e2})\frac{2E_{e1}E_{e2}-m_e^2}{E_{e1}E_{e2}}\right)\right)+\frac{6}{g_A^2}\left(3\epsilon_{GT}-\epsilon_F\right)\left(M^K_{GT}+M^L_{GT}\right)\right)\ .\end{aligned}\tag{2}$$

Setting $g_M=\epsilon_F=\epsilon_{GT}=0$ removes the the chiral contributions. With the pionic ϵ_F,ϵ_{GT} being:

$$\begin{aligned}\epsilon_F&=\frac{m_e g_V^2}{2F_\pi^2}\frac{1}{4\pi R_A}\left(M_F+\frac{m_\pi^2}{F_\pi^2}g^{NN}_{2\nu,F}M_{F,sd}\right)\ ,\\ \epsilon_{GT}&=\frac{1}{3}\frac{m_e g_A^2}{2F_\pi^2}\frac{1}{4\pi R_A}\left(M^{AA}_{GT}-2M^{AP}_{GT}+4M^{PP}_{GT}-\frac{3m_\pi^2}{g_A^2F_\pi^2}g^{NN}_{2\nu,GT}M_{F,sd}\right)\ .\end{aligned}\tag{3}$$

Here, $M_{F,sd}$ arises from the contact diagram, which cancels the singularities generated by the pion exchange diagrams [4, 8]. These NMEs were originally calculated for $0\nu\beta\beta$, where a massive "neutrino potential" is generated, consisting of a Klein-Gordon propagator multiplied by a rational function of $\mathbf{q}^2$. Similarly, the pion diagrams in figure 1 generate a chiral potential. This can be related to the neutrino potential by interpolating the paper's calculations and setting $m_\nu=m_\pi$.

One rough approximation we made is correcting for electromagnetic effects using the Fermi function $F(Z_f,E_{ei})$, with $Z_f=Z+2$. This assumes the nucleus is point-like, whereas more precise models including finite-size and screening, have shown this is accurate to within $\sim 10\%$ [10]. Future work ought to include these higher-order corrections.

Using both the Nuclear Shell Model (NSM, including g_A quenching) and the Quasi Particle Random Phase Approximation (QRPA) [1, 11], we compute the decay rate shown in table 1. We

	^{76}Ge QRPA	^{76}Ge NSM	^{136}Xe QRPA	^{136}Xe NSM
$T_0^{(2)}$	1.50	2.13	1.79	1.21
$T_\pi^{(2)}$	1.43	2.08	1.56	1.12
$T_{\mathrm{WM}}^{(2)}$	1.51	2.14	1.79	1.21
$T_\chi^{(2)}$	1.43	2.08	1.56	1.12

Table 1: Decay rates in units of 10^{21} yr. $T_0^{(2)}$ is the leading-order result. Subscripts indicate corrections included: π for pion exchange, WM for weak magnetism, and χ for both chiral corrections. The superscript (2) refers to the order of expansion as discussed in equations 6.

observe that the weak magnetic term has a relatively small effect, while the pion exchange diagrams dominate. This result is promising, especially since measuring the pion exchange contribution could help constrain $0\nu\beta\beta$, due to their similar NME structures. However, these results are currently limited by the aforementioned NME uncertainties, limiting this probe.

3. The Lepton Energy Expansion

We adopt the description of $2\nu\beta\beta$ from Šimkovic et al. [1] where:

$$M_{GT}^{K,L} = m_e \sum_n G_n \frac{\tilde{A}_n}{\tilde{A}_n^2 - \epsilon_{K,L}^2}, \ \tilde{A}_n = E_n - \frac{1}{2}(E_i + E_f), \ G_n = \langle 0_f^+ | \sum_k \vec{\sigma}_k \tau_k^+ | 1_n^+ \rangle \cdot \langle 1_n^+ | \sum_l \vec{\sigma}_l \tau_l^+ | 0_i^+ \rangle , \tag{4}$$

with $\tilde{A}_n$ the excitation energy, E_i, E_f the initial and final nucleon energies, and G_n the Gamow Teller NME, which dominates over the Fermi and tensor NMEs. The terms $\epsilon_{K,L}$ contain the lepton energies that tend to be smaller than $\tilde{A}_n$, allowing us to expand along the small $\epsilon_{K,L}/\tilde{A}_n$:

$$\epsilon_K = (E_{22} - E_{11})/2, \ \epsilon_L = (E_{12} - E_{21})/2, \ E_{ij} = E_{ei} + E_{\nu j} \ . \tag{5}$$

Performing this expansion including our NLO chiral correction:

$$\begin{aligned}
G_i^{2\nu} &= \frac{1}{\ln 2} \frac{(G_F V_{ud})^4}{8\pi^7 m_e^2} \int_0^Q \mathrm{d}\epsilon \int_{-\epsilon/2}^{\epsilon/2} \mathrm{d}\Delta \int_0^{Q-\epsilon} \mathrm{d}E_{\nu 1}\, E_{e1} |\mathbf{p}_{e1}| E_{e2} |\mathbf{p}_{e2}| E_{\nu 1}^2 E_{\nu 2}^2 \mathcal{A}_i , \\
\frac{d\Gamma}{d\epsilon} &= g_A^4 \left(M_{GT}^{(-1)} \right)^2 \Delta_0 \left[\frac{dG_0^{2\nu}}{d\epsilon} + \frac{dG_2^{2\nu}}{d\epsilon} \xi_{31} \frac{\Delta_2}{\Delta_0} + \frac{dG_4^{2\nu}}{d\epsilon} \left(\xi_{51} \frac{\Delta_2}{\Delta_0} + \frac{1}{3} \xi_{31}^2 \right) + \frac{dG_{22}^{2\nu}}{d\epsilon} \frac{1}{3} \xi_{31}^2 + \frac{dG_M^{2\nu}}{d\epsilon} \right] , \\
\Delta_0 &= 1 + \frac{4}{g_A^2} \frac{(3\epsilon_{GT} - \epsilon_F)}{M_{GT}^{(-1)}} - \frac{2 g_M}{3 m_N g_A} (Q + 2 m_e) \, , \Delta_2 = 1 + \frac{2}{g_A^2} \frac{(3\epsilon_{GT} - \epsilon_F)}{M_{GT}^{(-1)}} \, , \\
\mathcal{A}_M &= \frac{2 g_M}{3 m_N g_A} \frac{(E_{e1} + E_{e2})(2 E_{e1} E_{e2} - m_e^2)}{E_{e1} E_{e2}} \, ,
\end{aligned} \tag{6}$$

where we obtain the LO result by setting $g_M = 0$ and $\Delta_0 = \Delta_2 = 1$.

A benefit of this expansion is that it decouples the nuclear and the leptonic components. This is something we exploit with the shape factor S where the uncertain $g_A M_{GT}^{(-1)}$ cancels out:

$$S_i^{(m)} = \frac{1}{\Gamma} \frac{\mathrm{d}\Gamma}{\mathrm{d}\epsilon}, \ \delta S_i^{(m)} = S_i^{(m)} - S_0^{(m)}, \ \delta \bar{S}_i^{(m)} = \delta S_i^{(m)} / S_0^{(m)}, \tag{7}$$

PoS(MEDEX2025)004

where $m \in \{0, 1, 2, \ldots\}$ denotes the order to which we expand in $\tilde{A}_n/\epsilon_{K,L}$, and i indicates whether we are considering the uncorrected spectrum, the weak magnetism correction, the pion correction, or both combined (chiral correction), respectively $i \in \{0, \mathrm{WM}, \pi, \chi\}$. The expansion of Šimkovic et al. converges rapidly so we only go up to the second order. This cancellation of the front factor leaves the nuclear errors to the ξ_{31}, ξ_{51} factors which depends on G_N and $\tilde{A}_n$. In the figures 2 and 3, we plot the shape difference with respect to the approximate ξ_{ij} values (errors in the paper [7]):

$$\begin{aligned} {}^{76}\mathrm{Ge(QRPA)}:\ \xi_{31} = 0.11,\ \xi_{51} = 0.021, \quad {}^{136}\mathrm{Xe(QRPA)}:\ \xi_{31} = 0.32,\ \xi_{51} = 0.10, \\ {}^{76}\mathrm{Ge(NSM)}:\ \xi_{31} = 0.12,\ \xi_{51} = 0.022, \quad {}^{136}\mathrm{Xe(NSM)}:\ \xi_{31} = 0.16,\ \xi_{51} = 0.042\,. \end{aligned} \tag{8}$$

In figure 2, we show that high-precision fits for ξ_{31} and ξ_{51} need to include these corrections, as the higher-order terms in the expansion are of a similar order of magnitude as the chiral corrections. In figure 3, we show that the change in shape induced by weak magnetism dominates over that created by pion exchange, opposite to what we observed for the decay rates.

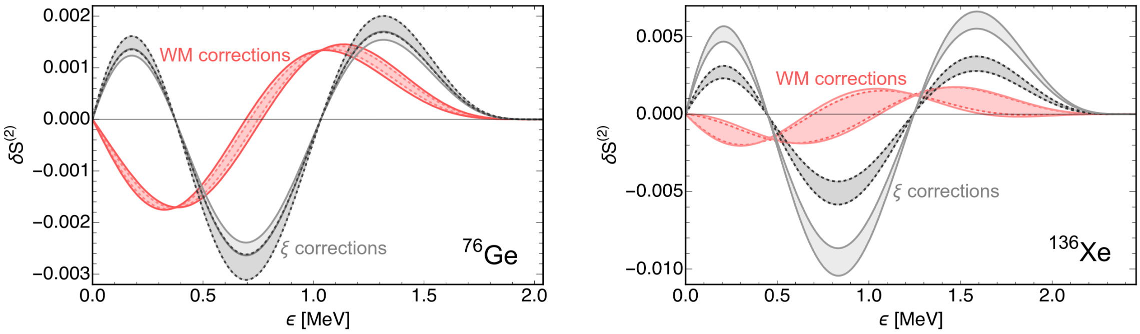

Figure 2: Change in spectrum for ^{76}Ge and ^{136}Xe from weak magnetism using values from table 8. We show results for both NSM (darker, dashed curves) and QRPA (lighter, solid curves).

4. Comparison to Sterile Neutrinos

When a sterile neutrino with a mass below the Q-value is included, we measure [9]:

$$\frac{d\Gamma'}{d\epsilon} = \left(1 - |V_{eN}|^2\right)\left[\left(1 - |V_{eN}|^2\right)\frac{d\Gamma}{d\epsilon} + 2\,|V_{eN}|^2\,\frac{d\Gamma^{\nu N}(m_N)}{d\epsilon}\right], \tag{9}$$

with sterile neutrino mass m_N and mixing angle V_{eN}. The rate $\Gamma^{\nu N}$, includes a light and massive sterile neutrino with modified phase space factor (equation 6). Setting $|V_{eN}|^2 = 0.1$ and $m_N = 1$ MeV in figure 4, values just at the limit of current constraints from $2\nu\beta\beta$ analyses, we observe that the chiral corrections are of a similar order of magnitude.

5. Conclusion

In this work, we analyzed chiral corrections to $2\nu\beta\beta$ decay. We computed leading $O(Q/\Lambda_\chi)$ contributions from weak magnetism, pion exchange, and short-distance two-body currents to the decay rate and spectrum, using the formalism of Šimkovic et al. for $2\nu\beta\beta$.

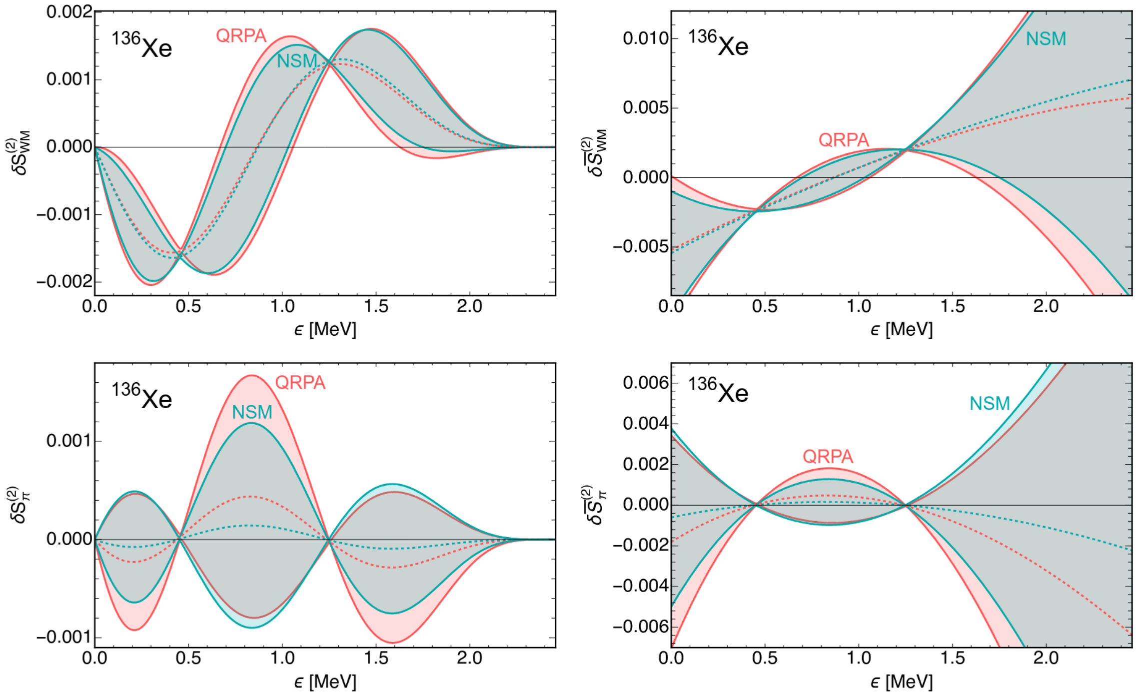

Figure 3: Corrections for ^{136}Xe from weak magnetism and pion contributions, using table 8's values.

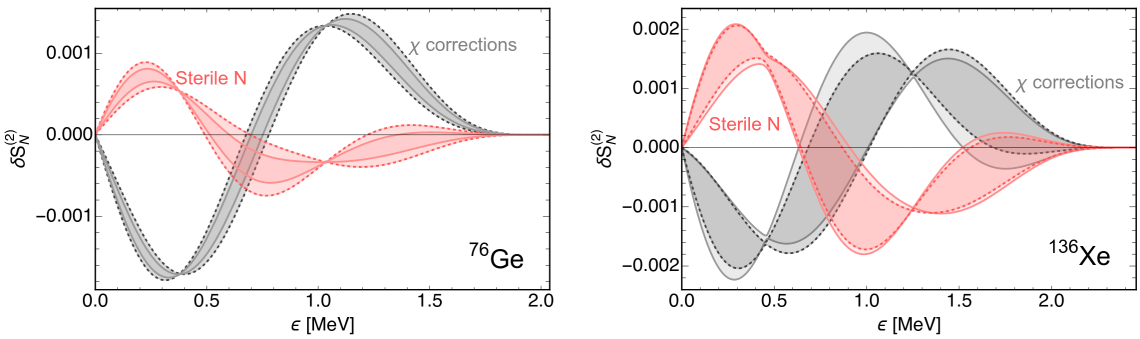

Figure 4: Shape-factor deviations δS_N stemming from chiral corrections in comparison with deviations introduced by a hypothetical sterile-neutrino contribution with mass m_N = 1 MeV and active–sterile mixing $|V_{eN}|^2 = 0.1$ for ^{76}Ge (left) and ^{136}Xe (right).

We showed that the total decay rate is reduced by several percent when chiral corrections are included, primarily due to pion exchange contributions, though nuclear structure uncertainties complicate their precise determination. We also demonstrated that the spectrum is modified, predominantly by weak magnetism, with distortions reaching the percent level.

These spectral effects should be accounted for in precision extractions of ξ_{31} and ξ_{51}, and are significant enough to impact certain BSM scenarios, such as models with sterile neutrinos [12, 13]. Future work should incorporate more comprehensive electromagnetic corrections and pursue improved *ab initio* predictions for $2\nu\beta\beta$ rates across isotopes.

References

[1] F. Šimkovic, R. Dvornický, D. Štefánik, and A. Faessler, *Improved description of the $2\nu\beta\beta$-decay and a possibility to determine the effective axial-vector coupling constant*, Phys. Rev. C **97**, 034315 (2018), doi:10.1103/PhysRevC.97.034315.

[2] N. Popara, A. Ravlić, and N. Paar, *Two-neutrino double-β decay matrix elements based on a relativistic nuclear energy density functional*, Phys. Rev. C **105**, 064315 (2022), doi:10.1103/PhysRevC.105.064315.

[3] V. Cirigliano, W. Dekens, J. de Vries, M. L. Graesser, and E. Mereghetti, *Neutrinoless double beta decay in chiral effective field theory: lepton number violation at dimension seven*, J. High Energ. Phys. **2017**, 082 (2017), doi:10.1007/JHEP12(2017)082.

[4] V. Cirigliano, W. Dekens, J. De Vries, M. L. Graesser, E. Mereghetti, S. Pastore and U. Van Kolck, Phys. Rev. Lett. **120** (2018) no.20, 202001 doi:10.1103/PhysRevLett.120.202001

[5] A. Belley, J. M. Yao, B. Bally, J. Pitcher, J. Engel, H. Hergert, J. D. Holt, T. Miyagi, T. R. Rodriguez and A. M. Romero, *et al.* Phys. Rev. Lett. **132** (2024) no.18, 182502 doi:10.1103/PhysRevLett.132.182502 [arXiv:2308.15634 [nucl-th]].

[6] A. Baroni, L. Girlanda, A. Kievsky, L. E. Marcucci, R. Schiavilla, and M. Viviani, *Tritium β decay in chiral effective field theory*, Phys. Rev. C **94**, 024003 (2016), doi:10.1103/PhysRevC.94.024003.

[7] S. e. Morabit, R. Bouabid, V. Cirigliano, J. de Vries, L. Gráf and E. Mereghetti, JHEP **06** (2025), 082 doi:10.1007/JHEP06(2025)082

[8] V. Cirigliano, W. Dekens, J. de Vries, M. Hoferichter and E. Mereghetti, Phys. Rev. Lett. **126** (2021) no.17, 172002 doi:10.1103/PhysRevLett.126.172002

[9] P. D. Bolton, F. F. Deppisch, L. Gráf, and F. Šimkovic, *Two-neutrino double beta decay with sterile neutrinos*, Phys. Rev. D **103**, 055019 (2021), doi:10.1103/PhysRevD.103.055019.

[10] J. Kotila and F. Iachello, *Phase-space factors for double-beta decay*, Phys. Rev. C **85**, 034316 (2012), doi:10.1103/PhysRevC.85.034316.

[11] W. Dekens, J. de Vries, D. Castillo, J. Menéndez, E. Mereghetti, V. Plakkot, P. Soriano, and G. Zhou, *Neutrinoless double beta decay rates in the presence of light sterile neutrinos*, J. High Energy Phys. **2024**, 9 (2024), doi:10.1007/JHEP09(2024)001.

[12] F. F. Deppisch, L. Gráf and F. Šimkovic, *Searching for New Physics in Two-Neutrino Double Beta Decay*, Phys. Rev. Lett. **125** (2020) no.17, 171801, doi:10.1103/PhysRevLett.125.171801.

[13] F. F. Deppisch, L. Gráf, W. Rodejohann and X. J. Xu, *Neutrino self-interactions and double beta decay*, Phys. Rev. D **102** (2020) no.5, 051701, doi:10.1103/PhysRevD.102.051701.